Signature of Anisotropy in Liquefiable Sand Under Undrained Shear

Jidong Zhao and Ning Guo

Abstract This paper presents a study on the anisotropic behavior of liqufiable sand subjected to undrained shear, by using a 3D Discrete Element Method with two different approaches describing particle rolling. By using a sliding and free-rolling model, the force network in relation to anisotropy in medium-loose or dense samples presents a clear bimodal character, while the liquefiable loose specimen behaves differently. Appreciable degree of anisotropy is found developed in the weak force network when the sample tends to liquefy. When the rolling resistance is considered, all samples show marked increases in anisotropy in both the weak and strong force networks as well as the overall shear strengths, as compared with the free-rolling case. The loose sample tends also to be more resistant to liquefaction in the latter case than in the free rolling case under otherwise similar conditions.

Keywords Granular sand • Liquefaction • Anisotropy • Discrete element method • Rotational resistance

1 Introduction

Granular anisotropy has been found playing a key role in the complex behavior of granular sand in response to external loads, such as strain localization and liquefaction failure, along with many other intriguing phenomena observed in sand. In particular, the problem of liquefaction in sand has attracted much attention due to its theoretical and practical significance. A proper understanding of the anisotropic behavior in liquefiable sand may shed light on deciphering the numerous puzzles concerning liquefaction such as its occurrence mechanism and post-liquefaction

J. Zhao (✉) · N. Guo
Department of Civil and Environmental Engineering, Hong Kong University of Science and Technology, Clearwater Bay, Kowloon, Hong Kong
e-mail: jzhao@ust.hk; ceguo@ust.hk

S. Bonelli et al. (eds.), *Advances in Bifurcation and Degradation in Geomaterials*, Springer Series in Geomechanics and Geoengineering 11,
DOI 10.1007/978-94-007-1421-2_6,

behavior (Jefferies and Been 2006). Available experimental tools, however, are practically limited in various ways to identify granular anisotropy and its evolution (Mitchell and Soga 2005). To this end, Discrete Element Method (DEM) offers a unique and convenient way for the study of granular anisotropy in sand from the grain level (Oda and Iwashita 1999), and will be adopted for the study. In this paper, a three-dimensional Discrete Element Method is employed to investigate the behavior of anisotropy in granular sand which develops deformation towards liquefaction. Two different approaches on particle rolling are compared. In particular, we examine the bimodal characteristic of force network in relation to granular anisotropy observed in (Azéma et al. 2007; Radjaï et al. 1998) for dense sand under drained shear. In the bimodal theory, it is found that the interparticle forces can be largely split into two networks, one with contacts of normal force greater than the average value and the other smaller than the average force. The former is called strong force network and the latter weak network. The two complimentary network differ from each other in a number of important ways in supporting the external load (for detail see Azéma et al. (2007) and Radjaï et al. (1998)).

2 Approach and Formulation

In the 3D DEM code used here, the interparticle sliding behavior is described by a linear force-displacement contact law, with the normal and tangential stiffnesses being set equal: $k_n = k_s = 10^5 N/m$ following (Oda and Iwashita 1999). The interparticle sliding is assumed to be governed by Coulomb's law and the coefficient of friction is set to $\mu = 0.5$. In addition to particle sliding, particle rolling has been found important in dictating the steric rearrangement of particles, and hence influences the macroscopic granular responses such as peak strength, dilation and liquefaction. In this study, we present two approaches handling the rolling case. The first considers free rotation of the particle body, i.e. the rolling is taken as a direct consequence of the inter-particle friction. The second approach takes into account particle rolling resistance by considering contact moment M_r (Ishihara and Oda 1998; Estrada et al. 2008). The interparticle contact is assumed to be plane-to-plane with a triangular distribution of normal force along the contact plane. A threshold moment is defined $M_{max} = \mu_r f_n l$ such that $|M_r| \leq M_{max}$, where μ_r denotes the coefficient of rolling resistance, and f_n is the normal force and l is a characteristic length related to the particle radii and the overlapping depth between particles (Guo and Zhao 2010). An assembly of 31,769 sphere particles with polydisperse radii ranged from 0.2 mm to 0.6 mm are randomly generated in a cube with rigid and frictionless bounding walls. It is then consolidated isotropically to reach different initial void ratio e_0 as shown in Table 1. These samples are then sheared under undrained condition which is achieved by adjusting the horizontal strain to keep the total volume of the assemblage constant with the major compression applied in the vertical direction. Note that no strain localization has been observed in the tested specimens. The stress tensor is defined as $\sigma_{ij} = \sum_{N_c} f_i^c d_j^c / V$, where V is the

Table 1 Initial properties and descriptions of samples for testing

Test	Label	e_0	Description
Series I	UL	0.644	Loose sample under undrained shear
	UM	0.634	Medium loose sample under undrained shear
	UD	0.612	Dense sample under undrained shear
Series II	UR0	0.644	Undrained shear with $\mu_r = 0.0$
	UR1	0.647	Undrained shear with $\mu_r = 0.1$
	UR3	0.648	Undrained shear with $\mu_r = 0.3$
	UR5	0.649	Undrained shear with $\mu_r = 0.5$

total volume of the assemblage, N_c is the total number of contacts, $\mathbf{f}^c$ is the contact force and $\mathbf{d}^c$ is the branch vector joining the centers of the two contact particles (Christoffersen et al. 1981). Stress quantities commonly used in triaxial tests are then obtained: $p' = \sigma_{ii}/3$, $q = \sqrt{3\sigma'_{ij}\sigma'_{ij}/2}$, where $\sigma'_{ij} = \mathrm{dev}(\sigma_{ij})$. Log-form strains are defined by the boundary displacements $\varepsilon_1 = \ln H_0/H$, $\varepsilon_v = \varepsilon_1 + \varepsilon_2 + \varepsilon_3 = \ln V_0/V$, where H_0 and V_0 are the initial height and volume of the assembly respectively (compression is taken as positive).

Two sources of anisotropy are considered: the geometrical anisotropy and the mechanical anisotropy (Satake 1982; Oda 1982; Ouadfel and Rothenburg 2001; Sitharam et al. 2009). The geometrical anisotropy is expressed in terms of the distribution of contact normals (and branch vectors if non-spherical particles are used), which is defined by the following fabric tensor:

$$\phi_{ij} = \int_{\Theta} E(\Theta) n_i n_j d\Theta, \quad E(\Theta) = \frac{1}{4\pi}\left[1 + a^c_{ij} n_i n_j\right] \tag{1}$$

where $\mathbf{n}$ is the unit contact normal vector, Θ is the solid angle in the spherical coordination system. Note that $a^c_{ij} = 15\phi'_{ij}/2$. The mechanical anisotropy in terms of normal force anisotropy and tangential force anisotropy are defined as follows:

$$\chi^n_{ij} = \frac{1}{4\pi}\int_{\Theta} \bar{f}^n(\Theta) n_i n_j d\Theta, \quad \bar{f}^n(\Theta) = \bar{f}^0[1 + a^n_{ij} n_i n_j], \tag{2}$$

$$\chi^t_{ij} = \frac{1}{4\pi}\int_{\Theta} \bar{f}^t(\Theta) t_i n_j d\Theta, \quad \bar{f}^t_i(\Theta) = \bar{f}^0[a^t_{ik} n_k - (a^t_{kl} n_k n_l) n_i], \tag{3}$$

where $\bar{f}^0 = \chi_{ii}^n$ is the average normal force. The second invariants of the three anisotropy tensors defined above are used to quantify the degree of anisotropy:

$$a_c = \sqrt{\frac{3}{2}a_{ij}^c a_{ij}^c}, \quad a_n = \sqrt{\frac{3}{2}a_{ij}^n a_{ij}^n}, \quad a_t = \sqrt{\frac{3}{2}a_{ij}^t a_{ij}^t} \tag{4}$$

A negative sign is attributed to a_c if the major principal direction of a_{ij}^c is more close to the perpendicular direction of the major principal stress direction, i.e., a_c has the same sign as $a_{ij}^c \sigma_{ij}'$.

3 Results and Discussion

Undrained triaxial compression tests are conducted with *free rolling* particles ($\mu_r = 0$) for Series I samples. The material responses are shown in Fig. 1. Note that the pore water pressure Δu is calculated by assuming a constant total confining pressure σ_3. As is shown, the three cases demonstrate perfectly the typical characteristic states a sand may experience, namely, peak strength (UM and UL), phase transformation state (UM and UD), liquefaction state (UL) and the critical state (UL and UD). The observations are in qualitative agreement with laboratory results (Mitchell and Soga 2005). The evolution of a_c and a_n in the strong/weak force subnetworks (Γ_{strong} and Γ_{weak}), and the entire force network (Γ_{total}) for UM and UL is shown in Fig. 2. The response of UD is similar to UM and will not be presented here. The anisotropic behavior of medium and dense samples (UM and UD) agrees favorably with the bimodal theory as found in (Radjaï et al. 1998). As is shown in Fig. 2a, c, the weak force network remains largely isotropic during the loading course (a_c is approximately zero and a_n is constantly small in the weak network during the loading course), whereas the strong force network is more anisotropically comprised of column-like chains which sustain nearly all deviatoric stress applied to the system. Note that the magnitude of a_t is small compared to

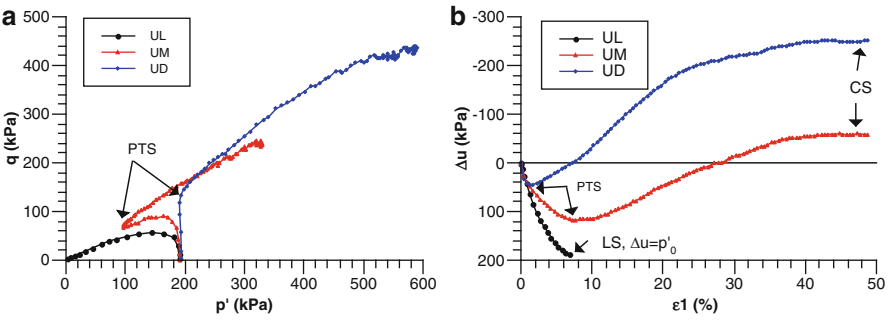

Fig. 1 Sand responses under undrained shear (**a**) $p' - q$; (**b**) $\varepsilon_1 - \Delta u$

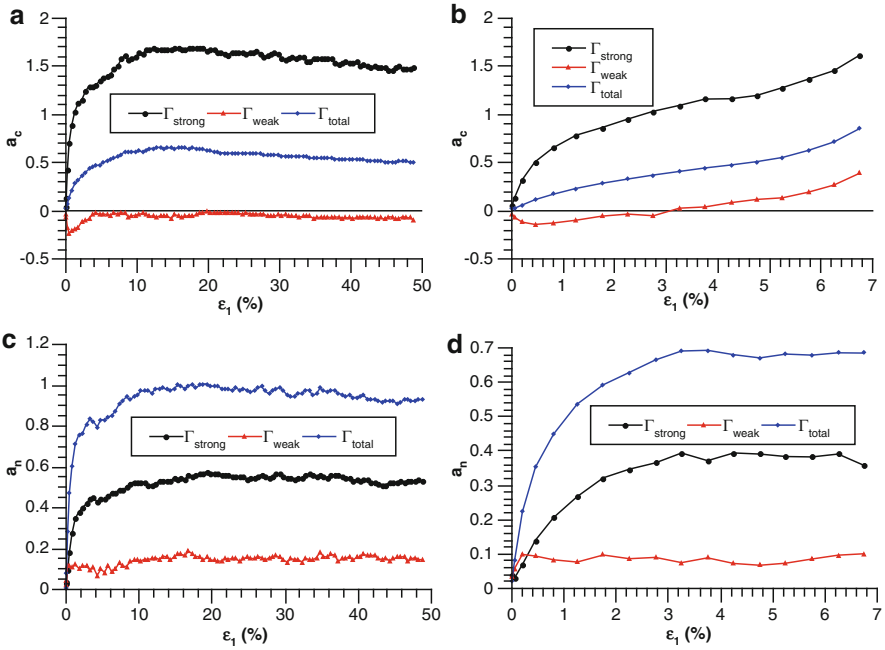

Fig. 2 Evolution of a_c and a_n for samples UM (**a, c**) and UL (**b, d**)

a_c and a_n, and are not presented here. As for the liquefiable loose sample UL, a_c in Γ_{weak} evolves gradually from a negative value to positive and finally reaches $a_c = 0.39$, which is very high compared to the cases of UM and UD. This indicates that in the loose case, the weak contacts have to sustain significant deviatoric loads due to the lack of efficient amount of strong force chain formed. This somehow may sacrifice its function of acting as the lateral support for the strong contact force columns. The overall structure may be more susceptible to abrupt buckling which leads to liquefaction. Though not presented here, it is meanwhile found that the (total) geometrical anisotropy contributes a much higher proportion to the overall strength in the UL case than in UM and UD, whereas in the latter two cases the mechanical anisotropy dominates the soil strength. Specifically, in the cases of UM and UD, a_n contributes more than 50% to the total strength and a_c contributes about 30%, whilst the tangential force anisotropy a_t contributes less than 20%. In the case of UL, the contributions from a_c and a_n are comparable. In some very loose cases a_c may even outweighs a_n in the shear strength. a_t remains at a very low proportion in all cases. For details see Guo and Zhao (2010).

The effect of rolling resistance on the undrained behavior of sand has also been examined by testing on samples in Series II in Table 1. Figure 3 shows the responses with different μ_r. It appears that the increase in μ_r generally leads to improved shear strength. Note that Samples UR0, UR1 and UR3 that are all otherwise regarded as loose and liquefiable in the free-rolling case manage to pull back their strength

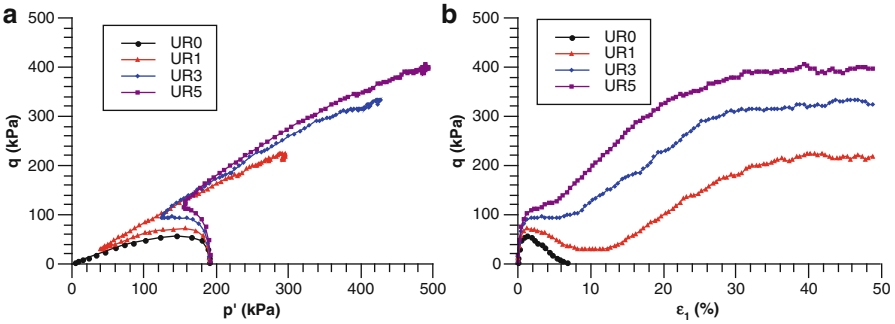

Fig. 3 Undrained behavior with rolling resistance: (**a**) p'-q; (**b**) ε_1-q

after reaching the phase transformation point. Liquefaction is observed only for the extremely loose case of UR5. It is also found that the critical state stress ratio in Series II is higher than that in Series I. This is reasonable as the rolling resistance generally leads to higher interlocking and higher internal friction angle for the samples. In the presence of rolling resistance, the distribution of anisotropy in the weak and strong networks is reminiscent to the case of free rolling case. Nevertheless, the magnitudes of a_c, a_n and a_t are greater than in the free rolling case, which explains the improved shear strength observed.

4 Conclusions

The behavior of anisotropy in a liquefiable sand under undrained shear has been studied using a three dimensional Discrete Element Method. Significant anisotropy is found in the weak force network when a loose sample is sheared towards liquefaction. Rolling resistance may generally help to increase the shear strength of a sand and to render a loose sand sample less vulnerable to be liquefied.

Acknowledgements This work was supported by RGCHK (Grant No. 622910, DAG08/09.EG04).

References

E. Azéma, F. Radjaï, R. Peyroux, Force transmission in a packing of pentagonal particles. Phys. Rev. E. **76**, 011–301 (2007)

J. Christoffersen, M.M. Mehrabadi, S. Nemat-Nasser, A micromechanical description of granular material behavior. J. Appl. Mech. **48**, 339–344 (1981)

N. Estrada, A. Taboada, F. Radjaï, Shear strength and force transmission in granular media with rolling resistance. Phys. Rev. E. **78**, 021–301 (2008)

N. Guo, J. Zhao, Characterization of granular anisotropy in sand under shear. J. Mech. Phys. Solids. Under review (2010)
K. Ishihara, M. Oda, Rolling resistance at contacts in simulation of shear band development by dem. J. Eng. Mech. **124**(3), 285–292 (1998)
M. Jefferies, K. Been, *Soil Liquefaction: A Critical State Approach* (Taylor & Francis, New York, 2006)
J. Mitchell, K. Soga, *Fundamentals of Soil Behavior*, 3rd edn. (John Wiley & Sons, New Jersey, 2005)
M. Oda, Fabric tensor for discontinuous geological materials. Soil. Found. **22**(4), 96–108 (1982)
M. Oda, K. Iwashita, *Mechanics of Granular Materials: An Introduction* (Taylor & Francis, Balkema/Rotterdam, 1999)
H. Ouadfel, L. Rothenburg, Stress-force-fabric relationship for assemblies of ellipsoids. Mech. Mater. **33**, 201–221 (2001)
F. Radjaï, D.E. Wolf, M. Jean, J.J. Moreau, Bimodal character of stress transmission in granular packings. Phys. Rev. Lett. **80**, 61–64 (1998)
M. Satake, Fabric tensor in granular materials, in *Deformation and Failure of Granular Materials*, ed. by P.A. Vermeer, H.J. Luger, A.A. Balkema, pp. 63–68 (1982)
T.G. Sitharam, J.S. Vinod, B.V. Ravishankar, Post-liquefaction undrained monotonic behaviour of sands: experiments and dem simulations. G*é*otechnique **59**(9), 739–749 (2009)